Electronic Supplementary Material (ESI) for Physical Chemistry Chemical Physics.

Supporting Information for: Is the Doped MoS_2 Basal Plane an Efficient Hydrogen Evolution Catalyst? Calculations of Voltage-Dependent Activation Energy

Sander Ø. Hanslin,[a,b] Hannes Jónsson,[b,c] and Jaakko Akola*[,a,d]

[a] *Department of Physics, Norwegian University of Science and Technology, NO-7491 Trondheim, Norway*

[b] *Faculty of Physical Sciences and Science Institute, University of Iceland, IS-101 Reykjavik, Iceland*

[c] *Applied Physics Department, Aalto University, FI-00076 Aalto, Finland*

[d] *Computational Physics Laboratory, Tampere University, FI-33101 Tampere, Finland*

* E-mail: jaakko.akola@ntnu.no

Supporting Information

Water Cluster Model

To assess convergence with respect to the explicit water description, reaction and activation energies obtained with the Hydronium (H_3O^+), Zundel ($H_5O_2{}^+$) and Eigen ($H_9O_4{}^+$) cations were compared. Cu-doped MoS_2 at zero initial hydrogen coverage was used for the comparison. As seen in Figure S1, the larger clusters generally lead to larger reaction and activation energies as the proton is stabilized. With respect to the Eigen cation results, the discrepancy with the Hydronium cation is at most 0.24eV, and with the Zundel cation at most 0.04eV. This indicates convergence as the coordination of the reacting water molecule is saturated. The calculations include also the implicit solvent, without which the proton becomes too unstable, as discussed in the main text. For the initial states, the water structure is optimized to a local minimum from the initial cation cluster configuration. The final states are obtained by locally optimizing the structure after the proton has been transferred. The transition states are then obtained as the peak of the minimum energy pathway between these structures, i.e. at the relevant saddle point between the two on the potential energy surface.

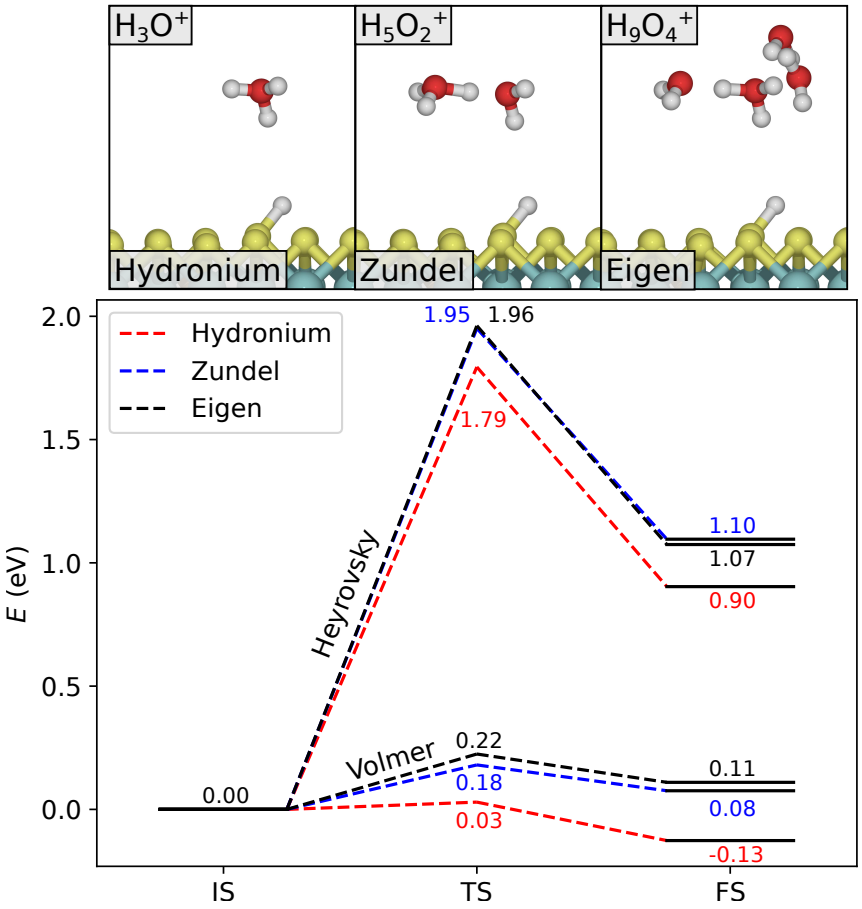

Figure S1: Reaction and activation energies obtained with different water cluster models are compared. Top panel shows the geometries for the Heyrovsky IS.

Local DOS

The localization of the induced S-p states are illustrated by Figure S2, where n denotes the group of atoms with similar distance from the dopant atom. We observe that for the early 3d-metals the contribution of higher-order nearest neighbors is significant relative to the $n = 0$ case, while for the later 3d-metals the contribution comes mainly from the $n = 0$ atoms. In addition, in the asymmetric cases of Co, Ni, Cu, we note that the most displaced $n = 0$ atom (denoted S*) carries a large part of the contribution. For Co and Ni it is the main contribution to high energy states below the Fermi level, but for Cu the contribution from other $n = 0$ atoms is also significant. In the symmetric or near-symmetric cases, such as Zn, the nearest neighbors contribute evenly. In short, the induced states are localized to a larger degree for the later 3d metals, and especially if the symmetry is broken.

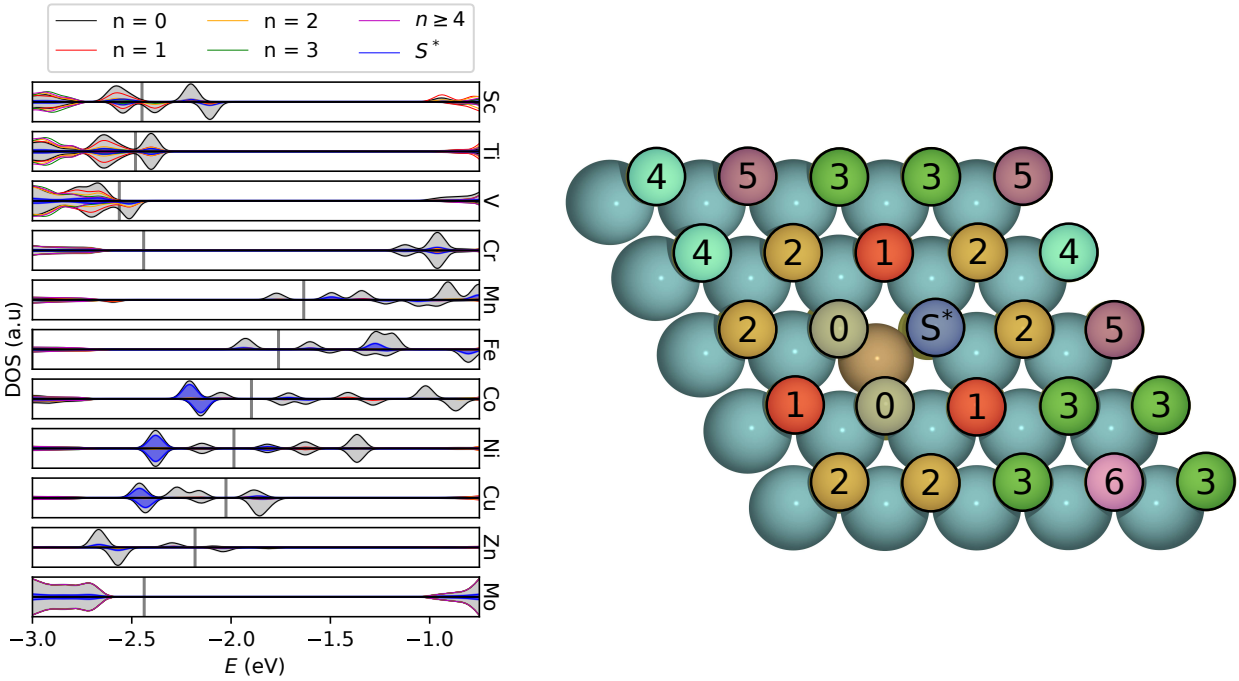

Figure S2: Left panel: Local density of doping-induced states projected onto S-p orbitals. Lines show the average of the n-th nearest neighboring S atoms. Blue fill shows the contribution of the most displaced atom (S*) in the $n = 0$ case. Right panel: Shows the groups of (nearly) symmetrically equivalent S-atoms in the Cu-doped 5×5 lateral supercell. S* is considered as part of $n = 0$.

Adsorption Sites

As shown in Figure S3, sites on the sulfur atoms neighboring the dopant atom are significantly more favorable than those further away. There is also some activation of these sites, and in the early 3d metals (Sc, Ti, V) the range-dependence is less pronounced. Still, the neighboring sites are most favored.

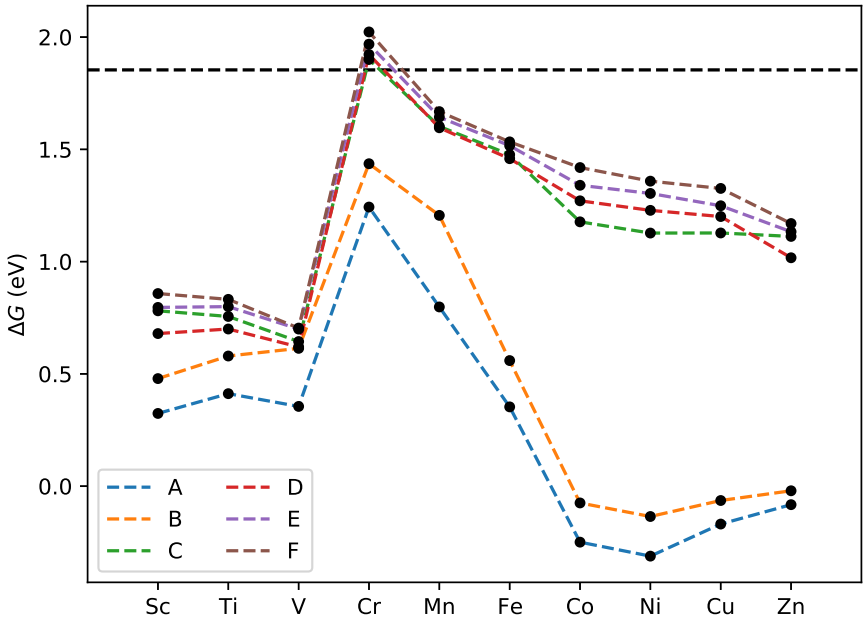

Figure S3: Free energies of adsorption onto the various sites for all the 3d metals. Site labels as given in Figure 4 for Cu-MoS_2. Dashed black line shows the MoS_2 reference. The late 3d metals have favorable sites near the dopant atom, the middle 3d metals have activated but unfavorable sites near the dopant atom, and the early 3d metals have activated but unfavorable sites both near and far from the dopant atom.

Hubbard U and Hybrid Functionals

The description of states in and around the gap for the 3d metals, and Mo itself, may be subject to errors due to the shortcomings of GGA with respect to describing localized and strongly correlated states. To verify the RPBE results we evaluate the DOS using the corrective DFT+U approach, as well with the hybrid functional PBE0. Applying the DFT+U approach, with $U = 3$eV for d-orbitals on the Mo and 3d-metals, the DOS is given in Figure S4. The main features remain, though in some systems the Fermi level (and surrounding features, e.g. the gap) is altered. The gap in pristine MoS_2 is not significantly changed.

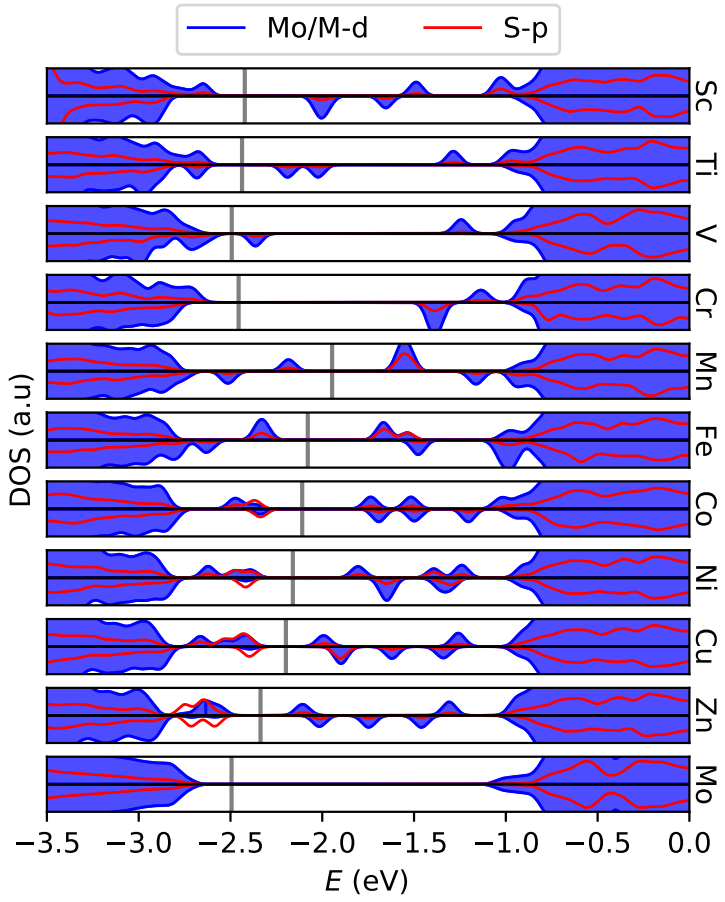

Figure S4: Density of states projected onto metal-d and S-p orbitals, using the Hubbard U correction with $U = 3$eV on Mo and 3d-metal d-orbitals. Comparing with Figure 3, features are mostly retained.

The effect of this on the promotion energy and adsorption energy is summarized in Figure S5, where the correlation is shown for the cases of RPBE, PBE+U ($U = 3$eV) and PBE0. The DFT+U approach only induces small changes in the energies, while the hybrid functional shifts the promotion energies upwards. The scaling relation is similar in all cases, indicating that for this purpose GGA is a sufficient level of theory to describe these properties in these systems.

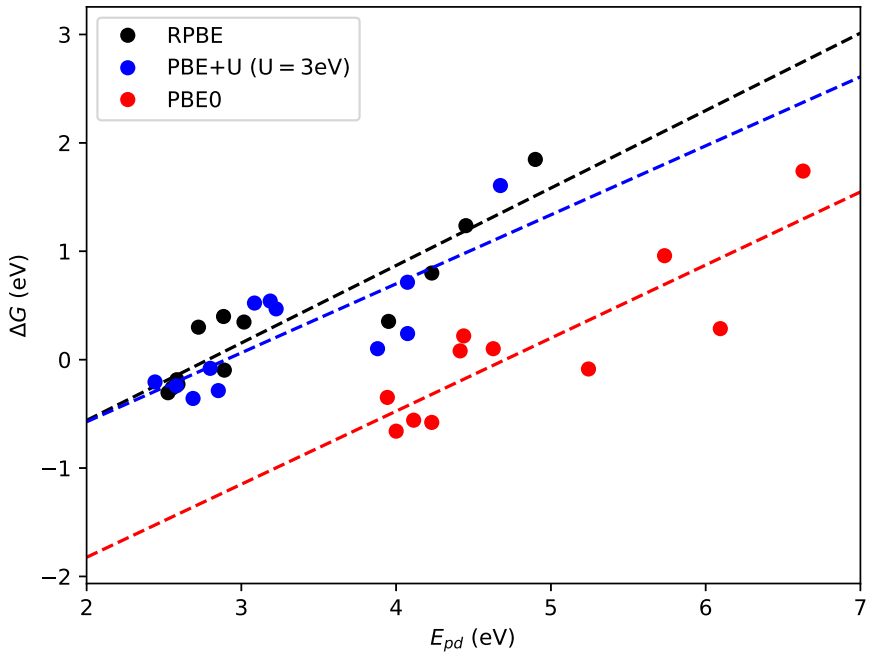

Figure S5: Correlation between promotion energy E_{pd} and adsorption free energy ΔG_{H} for the various approaches: RPBE, PBE+U and PBE0, along with linear fits. $U = 3$eV leads to only small changes in the energies with respect to the RPBE results, while PBE0 shifts the promotion energies towards higher levels. The trend and scaling slope is however maintained.

Tafel Mechanism

Figure S6 shows the adsorption free energy for some local minimum configurations on Cu-doped MoS_2. It is evident that the Cu-induced sites are still preferred despite H-H interaction. That is, configurations A-C combine the two most favorable single sites, leading to favorable 2 H-adsorption. Note that the geometry of C is very promising for Tafel desorption, and we suggest that the minimum energy reaction path from the most favorable A passes through C (and maybe B in the process) as an intermediate. From the energy of configuration D, it is clear that 2 H-adsorption on the same sulfur atom leads to strong interactions. The spread-out adsorption of configuration F is what one usually observes in uniform surfaces as a result of minimizing the H-H repulsion, which here is strongly unfavorable due to the low affinity of the pristine basal plane. Configurations E and G could have been interesting geometries for the Tafel reaction, but are likely limited by being too high in energy. Configurations A-D are clearly of interest for Tafel desorption.

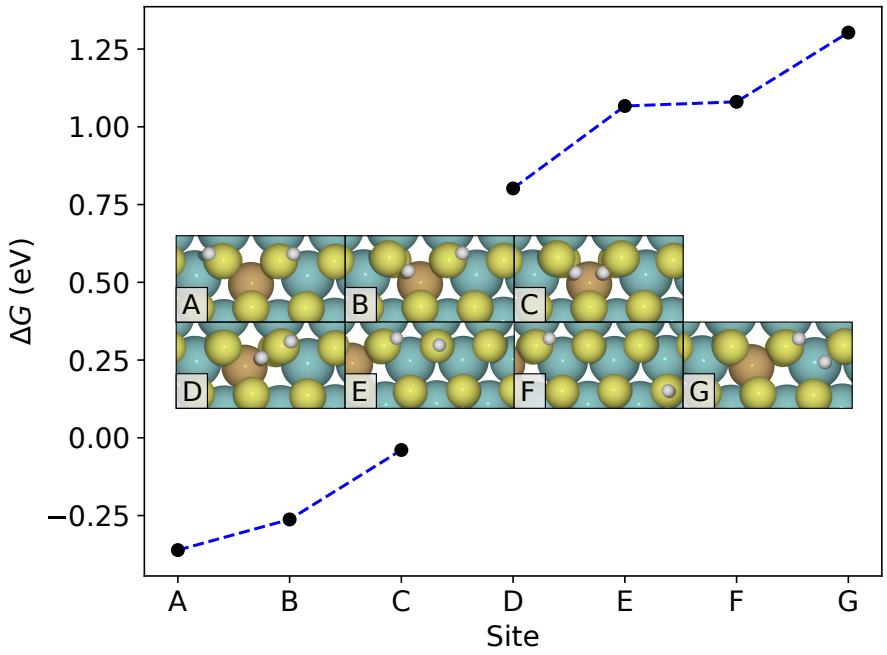

Figure S6: Adsorption energies for various configurations of two H-atoms on Cu-doped MoS_2.

Investigating the reaction paths, we find that the path A-B-C is preferred over A-B-D, and the former is shown in Figure S7. Further, Figure S8 shows the results for this reaction path for the relevant systems at coverage $\theta = 2/3$, along with the scaling relation. These calculations are performed in neutral cells and with the implicit solvent.

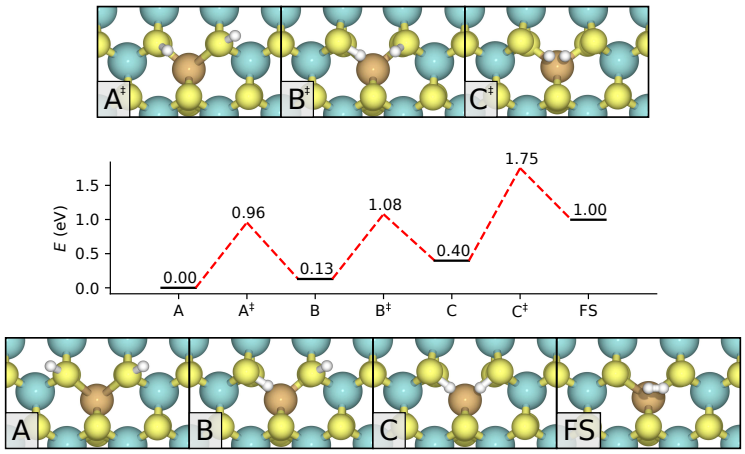

Figure S7: Preferred reaction path for the Tafel mechanism on Cu-doped MoS_2 at coverage $\theta = 2/3$. The corresponding transition states are shown in the top panel.

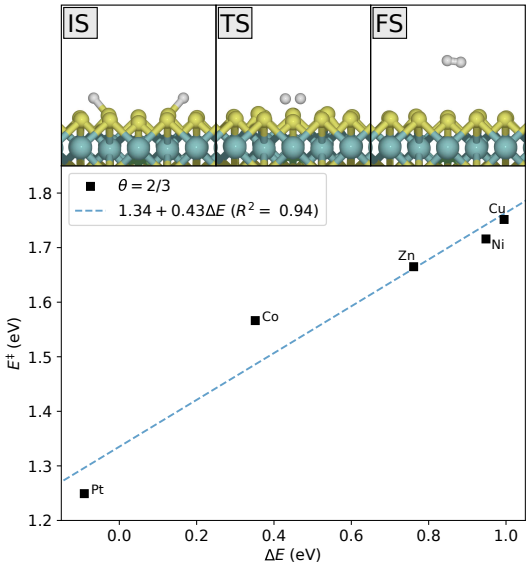

Figure S8: Top: Reaction mechanism for the Tafel reaction step on Ni-doped MoS_2 at an intial coverage of $\theta = 2/3$. Bottom: Calculated activation energy vs. reaction energy for the dopant systems which support nonzero equilibrium coverages at the potential of zero charge, and comparison with the Brønsted-Evans-Polanyi relation (dashed line).

Adsorption Energy Correlation

The correlation between adsorption energy $\Delta\Omega_{\mathrm{H}}$ and Heyrovsky barrier $\Omega_{\mathrm{h}}^{\ddagger}$ is used to construct the theoretical kinetic volcano. The linear fits are presented in Figure S9. As noted in the main text, the point outliers in this relation correspond to the outliers in the volcano. Deviations from this scaling relation directly leads to the different shape and peak position between the two volcanoes.

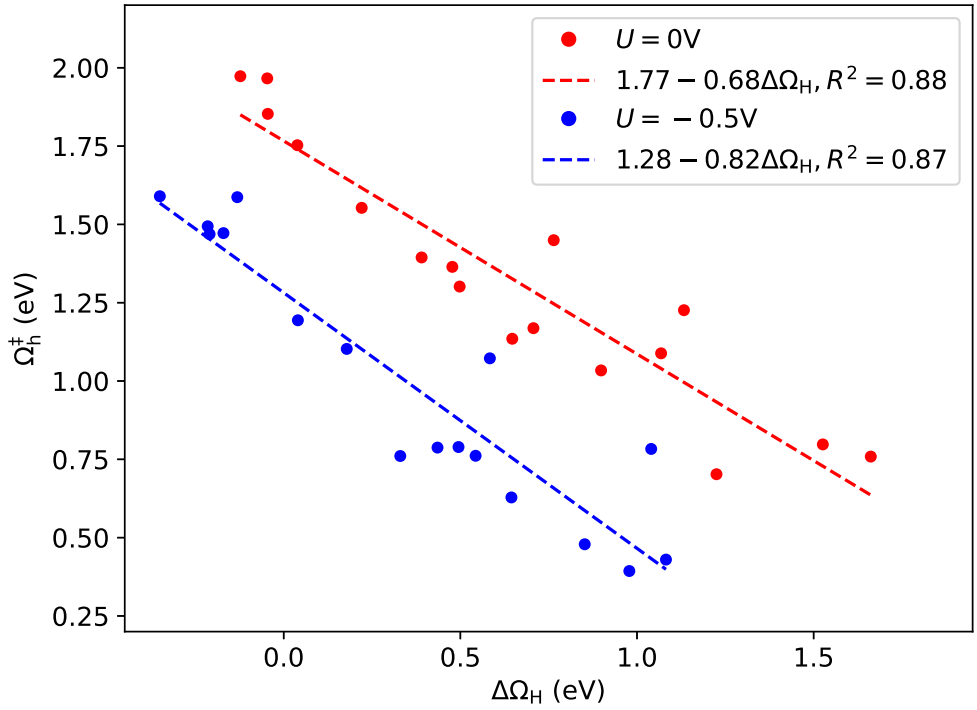

Figure S9: Correlation between adsorption energy $\Delta\Omega_{\mathrm{H}}$ and Heyrovsky barrier $\Omega_{\mathrm{h}}^{\ddagger}$ of all studied systems at $U = 0$V and $U = -0.5$V.